Lawrence Berkeley National Laboratory
Recent Work

Title
STATIC EQUILIBRIA OF THE INTERSTELLAR GAS IN THE PRESENCE OF MAGNETIC AND GRAVITATIONAL FIELDS: LARGE-SCALE CONDENSATIONS

Permalink
https://escholarship.org/uc/item/9cn8842v

Author
Mouschovias, Telemachos Ch.

Publication Date
1974-02-01

eScholarship.org Powered by the California Digital Library
University of California

Submitted to The Astrophysical Journal

RECEIVED
LAWRENCE
RADIATION LABORATORY

APR 24 1974

LIBRARY AND
DOCUMENTS SECTION

LBL-2681
Preprint

STATIC EQUILIBRIA OF THE INTERSTELLAR GAS IN THE PRESENCE OF MAGNETIC AND GRAVITATIONAL FIELDS: LARGE-SCALE CONDENSATIONS

Telemachos Ch. Mouschovias

February 1974

Prepared for the U. S. Atomic Energy Commission
under Contract W-7405-ENG-48

TWO-WEEK LOAN COPY

This is a Library Circulating Copy which may be borrowed for two weeks. For a personal retention copy, call Tech. Info. Division, Ext. 5545

LAWRENCE BERKELEY LABORATORY • UNIVERSITY OF CALIFORNIA •

LBL-2681
c.2

DISCLAIMER

This document was prepared as an account of work sponsored by the United States Government. While this document is believed to contain correct information, neither the United States Government nor any agency thereof, nor the Regents of the University of California, nor any of their employees, makes any warranty, express or implied, or assumes any legal responsibility for the accuracy, completeness, or usefulness of any information, apparatus, product, or process disclosed, or represents that its use would not infringe privately owned rights. Reference herein to any specific commercial product, process, or service by its trade name, trademark, manufacturer, or otherwise, does not necessarily constitute or imply its endorsement, recommendation, or favoring by the United States Government or any agency thereof, or the Regents of the University of California. The views and opinions of authors expressed herein do not necessarily state or reflect those of the United States Government or any agency thereof or the Regents of the University of California.

STATIC EQUILIBRIA OF THE INTERSTELLAR GAS IN THE PRESENCE OF MAGNETIC AND GRAVITATIONAL FIELDS: LARGE-SCALE CONDENSATIONS*

TELEMACHOS CH. MOUSCHOVIAS

Physics Department, University of California, Berkeley

and

Harvard College Observatory, Cambridge, Massachusetts

*This work was supported mainly by the National Science Foundation under grant GP 36194X, and in part by the Lawrence Berkeley Laboratory under the auspices of the U. S. Atomic Energy Commission.

ABSTRACT

We present equilibrium states of the interstellar gas, which has run down the perturbed magnetic field lines of a stratified, isothermal initial state under the action of a vertical galactic gravitational field. The final states are lower in total energy than the corresponding initial states. Their properties depend quantitatively on the horizontal (but not so much on the vertical) wavelength of the initial perturbation. A striking feature of the final states is that the scale-height of the gas increases (decreases) where the gas density increases (decreases). A connection between initial and final states is made by conserving the mass-to-flux ratio in each flux tube. Thus, although we determine final equilibrium states by solving a time-independent problem, in a time-dependent problem our final states can be reached from the corresponding initial states through continuous deformations of the field lines. The final states are consistent with observations in the solar neighborhood. We treat the interesting case of the magnetic pressure being initially comparable to the pressure of the thermal gas.

We show that the isothermal gas-field-gravity system possesses an "energy integral". An effective potential energy is identified, and an "energy principle" follows as a corollary. The iterative procedure used in order to solve the magnetohydrostatic equations is outlined, and upper limits on the numerical errors are given. We also extend our formalism so that it can apply to the case of a general (rather than an isothermal) equation of state.

Running title: Interstellar Gas and Field

Subject Headings: hydromagnetics - instabilities - interstellar matter - magnetic fields - plasmas

I. INTRODUCTION

The dimensions of many condensations of the interstellar gas are so large and the condensations themselves are so closely associated with the interstellar magnetic field that one may conclude that these large-scale condensations could be produced by very long-wavelength hydromagnetic disturbances. Parker (1966) showed, using linear stability analysis, that the interstellar gas, which is partially supported by magnetic and cosmic-ray pressures against the Galactic gravitational field, could be unstable with respect to deformations of the field lines. Lerche (1967a) determined a final state for the interstellar gas and field system, in which Parker's magnetogravitational instability had developed. Since he ignored the pressure of the gas, the final state consisted of infinitesimally thin sheets of matter that extended perpendicular to the galactic plane. This state is unstable with respect to small horizontal displacements of the gas elements (Lerche 1967b). Parker (1968a) found a different equilibrium state, but at the same time he pointed out the very special nature of his solution because of a simplifying mathematical assumption made (see §IIa below).

In this paper we assume strict flux-freezing and we derive a general non-linear, elliptic, second-order, partial differential equation, a subset of whose solutions properly describes equilibrium states of the interstellar gas and field system in a galactic gravitational field (§IIa). In §IIb, by making use of constants of the motion, we remove an arbitrariness that would otherwise exist in the source term of this equation. This allows us to make a connection between initial and final states, even though we solve a time-independent problem. The boundary conditions and the assumed initial state are presented in §III. In §IV we obtain and discuss an "energy integral" of the isothermal gas-field-gravity system and we endeavor to anticipate what

energy changes will take place as the system makes a transition from an initial to a final state. The physics corresponding to each step of the method of solution is explained in §Va. Indications for the physical stability of the final states are discussed in §Vb. We present three typical final states in §VI; important features and observational predictions are discussed in some detail. In §VII we make a few concluding remarks and a semi-quantitative comparison with observations in the solar neighborhood. Mathematical derivations, that would interrupt the continuity of an argument, and a description of our iterative scheme are left for the appendices. The generalization of our formalism, so that it can apply to equations of state $P = P(\rho)$, is also left for an appendix.

II. HYDROSTATIC EQUILIBRIUM INCLUDING FLUX-FREEZING

a) Reduction to one equation

Consider a conducting gas of density ρ and pressure P in hydrostatic equilibrium in a magnetic field $\vec{B}$ and a gravitational field $\vec{g}$, derivable from a potential ψ. Denoting the current density by $\vec{j}$, we may write the magneto-hydrostatic force equation as

$$-\vec{\nabla}P - \rho\vec{\nabla}\psi + \vec{j}\times\vec{B}/c = 0, \tag{1}$$

where c is the speed of light in vacuum. The quantities $\vec{B}$ and $\vec{j}$ are related by Maxwell's equation

$$c\vec{\nabla}\times\vec{B} = 4\pi\vec{j}. \tag{2}$$

The equation of state is

$$P = \rho C^2, \tag{3}$$

where C is the isothermal speed of sound in the gas. In this paper we take C = constant. If a magnetic vector potential, $\vec{A}$, is defined by

$$\vec{B} = \vec{\nabla}\times\vec{A}, \tag{4}$$

Maxwell's equation

$$\vec{\nabla}\cdot\vec{B} = 0 \tag{5}$$

is satisfied identically.

Following previous authors, we assume that all quantities are independent of z (2D geometry) and that $B_z = 0$. Then $B_x = +\partial A/\partial y$, $B_y = -\partial A/\partial x$ and the magnetic vector potential can be written as $\vec{A} = \vec{e}_z A(x,y)$. Since $\vec{B} = -\vec{e}_z\times\vec{\nabla}A$, it follows that $\vec{B}\cdot\vec{\nabla}A = 0$ and, therefore, that A is constant on a field line. Assuming flux-freezing one can show that $\vec{v}\cdot\vec{\nabla}A = 0$, so that A is a constant of the motion in the flow associated with Parker's instability. Each field line, therefore, retains its initial value of A.

We define a scalar function of position, q(x,y), by

$$q = P\ \exp(\psi/C^2) \tag{6}$$

and we write equation (1) in terms of A and q as

$$j\vec{\nabla}A/c = \exp(-\psi/C^2)\ \vec{\nabla}q. \tag{7}$$

Decomposing equation (7) in directions parallel and perpendicular to field lines and recalling that A is constant on a field line, we can show that

$$P\ \exp(\psi/C^2) \equiv q = \text{constant on a field line} = q(A); \tag{8}$$

and that

$$\frac{j}{c}\ \exp(\psi/C^2) = \text{constant on a field line} = \frac{dq}{dA}. \tag{9}$$

The quantity q, being a function of A at hydrostatic equilibrium, expresses the fact that, since magnetic forces act only perpendicular to the field lines, pressure gradients exactly balance the gravitational forces along a field line. The meaning of equation (9) is as follows. If a magnetic vector potential $A^*(x,y)$ [and, therefore, a magnetic field $B^*(x,y)$] is given, and if matter is distributed among field lines so that the forces parallel to field lines are in exact balance [i.e., $q^* = q^*(A^*)$], then we can balance the forces in a direction perpendicular to the field lines by calculating a current density j^* from equation (9). However, B^* and j^* will not be consistent with each other, unless they satisfied equation (2), which may be written in terms of A, with j eliminated in favor of q, as

$$\nabla^2 A = -4\pi \frac{dq}{dA} \exp\left(-\frac{\psi}{c^2}\right). \qquad (10)$$

So far, equation (10) differs from an equation derived by Dungey (1953) only in that our ψ is any gravitational potential. For example, ψ can be the gravitational potential of the Galaxy as a whole, or that of a dense cloud in the interstellar medium. In the former case, ψ can be obtained from Schmidt's (1965) model of the Galaxy; in the latter case, a Poisson equation for ψ has to be considered simultaneously with equation (10) in order to obtain a self-consistent solution. In this paper we take ψ to be due to the Galaxy as a whole.

Let the gas and field system be in some initial state, in which Parker's (1966) magnetogravitational instability develops with wavelengths λ_x and λ_y in the x- and y- directions, respectively. We take the system to be periodic in x (along the galactic plane) and we assume that the pair of (unstable) wavelengths (λ_x, λ_y) is the same everywhere in the galaxy. Moreover, we assume that the magnetic field is frozen in the matter. In order to find a final

equilibrium state for this system we must solve equation (10); and for this task we need to calculate q(A). Parker (1968a) assumed that q(A) is either a linear, or a quadratic function of A, and he solved the resulting linear equation (10) for the case in which the gravitational potential, ψ, is proportional to the vertical distance, y. We find below that, for the plane-parallel initial state proposed by Parker (1966), the function q varies as an inverse power of A [see equation (15)]. In the final states as well, q varies as some inverse power of A (see Figure 1). Although q is a function of A alone at hydrostatic equilibrium, it is not a constant of the motion. Consequently, we are not permitted to calculate (or to specify) q(A) in some initial state and then procede to determine a final state characterized by the same q(A).

b) Calculation of the function q(A)

In general, q(A) can be calculated as follows. With $X \equiv \lambda_x/2$, the mass (δm) in a flux tube between field lines characterized by A and A+δA is, by definition,

$$\delta m(A) = \int_{-X}^{+X} dx \int_{y(x,A)}^{y(x,A+\delta A)} dy(x,A)\ \rho(x,y(x,A)). \qquad (11)$$

It is natural to consider x and A as the independent variables. Since the integration over y in equation (11) is performed keeping x fixed, we may write $dy = dA\ (\partial y/\partial A)$ and effect the change of variables from y to A. We eliminate ρ in favor of A by using equations (8) and (3), and we expand the integrand of the resulting equation in a Taylor series about A keeping only first-order terms. (Neglecting higher-order terms is justified a posteriori.) We then solve for q(A) to obtain

$$q(A) = \frac{C^2}{2}\frac{dm}{dA} \Big/ \int_0^X dx\ \frac{\partial y(x,A)}{\partial A}\ \exp\left[-\frac{\psi(x,A)}{C^2}\right]. \qquad (12)$$

The quantity y(x,A) refers to the y-coordinate of the field line A at x.[1]

---

[1] In Appendix A we generalize the definition of q [equation (6)] to apply to any equation of state, $P = P(\rho)$. We also derive equations, which are generalizations of equations (10) and (12).

If dm/dA is given, q(A) follows from equation (12) for any proposed configuration. In particular, both q for the initial and q for the final states can be calculated using the same dm/dA, since conservation of both mass and flux implies that dm/dA is a constant of the motion.

Note that q(A) depends on the shape of the field lines, which are originally unknown. Hence, in general, one must solve equations (10) and (12) simultaneously for any given dm/dA. The initial state of the gas and field system is not known in reality, for it depends on the mechanism which creates the magnetic flux. Here we take it to be the plane-parallel system proposed by Parker (1966). This defines dm/dA for the final state as well. We emphasize, however, that the only information needed in order to determine a final state is the mass-to-flux ratio in each flux tube. If the distribution of mass among the various flux tubes is obtained from observations, we can determine a final equilibrium state without reference to any particular initial state.

III. THE INITIAL STATE - BOUNDARY CONDITIONS

As an initial state we consider the stratified equilibrium state of the interstellar gas and magnetic field in a gravitational field $\vec{g} = -\vec{e}_y g(y)$, where $g(y) = -g(-y) =$ a positive constant. Following Parker (1966), we assume that the ratio of the magnetic-to-gas pressures,

$$\alpha \equiv B^2/8\pi P, \tag{13}$$

is constant in the initial state. For this state we find

$$A_i(y) = -2HB_i(0)\ \exp(-y/2H)\ , \tag{14}$$

$$q_i(A_i) = \rho_i(0)\ C^2\ \left(-2HB_i(0)/A_i\right)^{2\alpha} \tag{15}$$

and

$$\frac{dm}{dA} = \frac{2X\rho_i(0)}{B_i(0)}\ \left(-\frac{A}{2HB_i(0)}\right)\ , \tag{16}$$

where $X \equiv \lambda_x/2$ and H is the combined scale-height of the gas and field given by

$$H \equiv (1+\alpha)C^2/g\ . \tag{17}$$

The quantities $B_i(0)$ and $\rho_i(0)$ are, respectively, the values of B_i and ρ_i at $y = 0$. The subscript i signifies the initial state. In equation (16) A is not subscripted because, as explained in §IIb, dm/dA is the same function of A in the initial and final states.

The boundary conditions are as follows. Since the x-axis is taken to coincide with the galactic plane and the system is assumed periodic in x, there is reflection symmetry about both the x- and the y-axes. The former symmetry implies that the field line originally coinciding with the x-axis remains undeformed, i.e.,

$$A(x,y=0) = -2HB_i(0) = \text{constant}. \tag{18}$$

Periodicity in x is expressed by

$$\left.\frac{\partial A(x,y)}{\partial x}\right|_{x=0,\pm X} = 0\ . \tag{19}$$

Boundedness at infinity and conservation of the total magnetic flux imply

$$A(x,y) = \begin{cases} 0, & y = +\infty \\ -4HB_i(0), & y = -\infty \end{cases} . \tag{20}$$

Because of the symmetries, equation (10) may be solved in the rectangle $0<x<X$, $0<y<\infty$. In fact this semi-infinite rectangle may be replaced by a finite one without affecting the solution very much, provided only that the extent of the finite rectangle in the y-direction is much larger than H (see §VId). So, we set the upper boundary at $y = Y >> H$ and we replace equation (20) by

$$A(x,y) = A_i(Y) , \tag{21}$$

where $A_i(Y)$ is the initial value of A at $y = Y$. Recalling that the perturbations which Parker (1966, Appendix III) showed to be unstable, always leave some field lines of the initial state undeformed, equation (21) is equivalent to taking the upper boundary at the position of the first undeformed field line of the initial state.

Before solving equations (10) and (12) we wrote them in a dimensionless form (see Appendix C1). Thus, α of the initial state is the only free parameter in the equations (see equation C1, Appendix C).

IV. ENERGY CONSIDERATIONS

a) An Energy Principle

In Appendix B we show that the magnetohydrodynamic equations possess an "energy integral", and we identify an effective potential energy (W) of the isothermal gas-field-gravity system which is given by

$$W = W_p + W_m + W_g , \tag{22}$$

where

$$W_p = \int P \ln P \, dV , \tag{23}$$

$$W_m = \int (B^2/8\pi)\, dV \quad \text{and} \quad W_g = \int \rho\psi\, dV \,. \qquad (24), (25)$$

One can show directly that the force equation (1) follows from the requirement that the first variation of W vanish under an arbitrary displacement $\vec{\xi}$ of the plasma elements, provided that: (i) mass is conserved; (ii) flux is conserved; (iii) the temperature is constant. In the case of a system periodic in one direction (x), one needs the additional assumption that (iv) no mass is transferred from one period to the next during the infinitesimal plasma displacements. This demonstration rigorously qualifies W as a potential energy and allows one to study the stability of an equilibrium state by investigating the sign of the potential energy associated with small deviations from the assumed equilibrium.

b) The Meaning of W_p

In equation (22), the magnetic energy (W_m) and the gravitational energy (W_g) are given by familiar expressions. Note, however, that the quantity $P \ln P$ has replaced the usual term $P/(\gamma-1)$. The meaning of $P \ln P$ becomes transparent, if we examine the first law of thermodynamics (for an ideal gas in the absence of any fields). This is

$$dQ = du + P\, d(\rho^{-1}) \,. \qquad (26)$$

The quantities Q and u are, respectively, the heat supplied to the gas and the internal energy of the gas; both Q and u are measured in units of energy per unit mass. For an isothermal process du vanishes and dQ is an exact differential.

Letting θ denote the heat per unit volume supplied to the gas (i.e., $\theta = \rho Q$), we may write equation (26) as

$$d\theta = \left(\frac{\theta}{P} - 1\right) dP \ . \tag{27}$$

A straight-forward integration yields θ as a function of P; this is further integrated over volume to obtain

$$\begin{aligned} \Theta &\equiv \int \theta \, dV \\ &= - \int P \ln P \, dV + b \int P \, dV \\ &= - W_p + b \int P \, dV \ , \end{aligned} \tag{28}$$

where b is a constant of integration. The second term in the right-hand side of equation (28) is the same for all states, because the total mass is fixed and the gas is isothermal. Therefore, the heat ($\Delta\Theta$) supplied to the gas in going from one state to another, is simply given by

$$\Delta\Theta = - \Delta W_p \ . \tag{29}$$

Since ΔW_p was derived from the second term in the right-hand side of equation (26), it represents the work done by the gas against pressure forces in making a transition between two states along an isothermal path. If $\Delta W_p > 0$, heat is released by the gas. Note, also, that for a reversible isothermal process, the change in the entropy (denoted by ΔS) is given by

$$\Delta S = \Delta\Theta/T = - \Delta W_p/T \ . \tag{30}$$

Hence, W_p provides a measure of the entropy and it is equal to the Helmholtz free energy of the gas, to within an additive constant.

c) Expected Energy Changes

When Parker's instability develops, compression occurs in some parts of the system and expansion in others. Consequently, one cannot anticipate what the net changes in W_m and W_p will be when a final state is reached. Compression (expansion) tends to increase (decrease) W_m and W_p. This is obvious in the case of W_m. It is so for W_p as well because, when gas is being compressed it tends to heat up; for the temperature to remain constant (an assumption in our model), heat has to be released. Typical cooling times are of the order of 10^5 years in the interstellar medium and become shorter as the gas density increases (Spitzer 1968). Since this time is smaller than the e-folding time of the instability (10^7 years), the gas has enough time to cool down.

The gravitational energy (W_g) is expected to decrease, since gas drains down the perturbed field lines under the action of the galactic gravitational field. The "fact" that the expanding field lifts some matter to higher altitudes is not expected to produce a net increase in the gravitational energy, for field lines can expand only because gas is being "unloaded" from their raised portions.

V. METHOD OF SOLUTION AND PHYSICAL STABILITY

a) The Physics Behind the Method of Solution

To obtain a simultaneous solution of the equilibrium equations (10) and (12) we developed and followed the procedure outlined in Appendix C. The physics behind that iterative procedure is as follows. (i) Guess a set of field lines (and, therefore, a magnetic field), which satisfy the periodicity and symmetry conditions discussed in §III. (ii) Distribute the total mass among the various flux tubes in such a way, that the mass-to-flux ratio in each flux tube is equal to the mass-to-flux ratio in the corresponding flux

tube of the initial state. (iii) Allow mass to slide up or down along field lines (without transferring any mass from one tube to another) until pressure gradients and gravitational forces are in exact balance along field lines. (iv) From the magnetic field obtained in step (i) and the mass distribution achieved in step (iv), calculate the current density necessary to balance all forces in a direction perpendicular to the field lines. (v) Check whether the just calculated current density is consistent with the magnetic field of step (i); if it is not, use this current density to calculate a new ("better") magnetic field and go to step (ii) to repeat the process until consistency is achieved. The introduction of an underrelaxation parameter in the iterative scheme provides a measure of how much "better" (or "worse"!) the magnetic field of one iteration is, compared to that of the previous iteration.

b) Stability

The stratified initial state is unstable only if the horizontal and vertical wavelengths of the applied perturbation simultaneously exceed some critical values (see Parker 1966), namely,

$$\lambda_x > \Lambda_x \equiv 4\pi H(2\alpha+1)^{-1/2} \quad , \quad \alpha \neq 0 \tag{31}$$

and

$$\lambda_y > \Lambda_y(\lambda_x) \equiv \Lambda_x(1-\mu^2)^{-1/2} \quad . \tag{32}$$

The quantities α and H are defined by equations (13) and (17), respectively, and $\mu = \Lambda_x/\lambda_x < 1$. Parker's dispersion relation implies that, for a fixed $\lambda_x > \Lambda_x$, the growth-rate of the perturbation increases as λ_y ($>\Lambda_y$) increases.

In addition, for a fixed $\lambda_y > \Lambda_y$, the growth-rate first increases and then decreases as λ_x increases. The maximum growth-rate is reached when $\lambda_x \lesssim 2\Lambda_x$ and $\lambda_y = \infty$. For typical parameters of the interstellar medium, the inverse of the maximum growth-rate is, approximately, 10^7 years. This is smaller than the time required for one galactic rotation (approximately 10^8 years).

Starting from the stratified initial state, we applied a perturbation (in the form of a deformation of the field lines) characterized by a stable pair of wavelengths (λ_x,λ_y). Our iterative scheme always converged to the initial state, no matter how large the amplitude of the perturbation was and regardless of the particular values of λ_x and λ_y, as long as they were stable. On the other hand, our iterative scheme never converged to the initial state in the case that the perturbation was characterized by an unstable pair of wavelengths, even if the amplitude of the perturbation was as small as 1%. This is an indication (although not a proof) that the iterative scheme cannot converge to solutions representing physically unstable states.

For a fixed unstable pair of wavelengths, we obtained convergence to one and the same solution (distinct from the initial state) for a wide range of amplitudes of the initial perturbation. When perturbations were applied to this solution, the iterative scheme always converged back to it. This, in conjunction with the properties of the iterative scheme described in the proceding paragraph, suggests that our solutions represent states of the gas-field-gravity system which are physically stable, at least in a local sense. The class of perturbations applied to a final state was such, that each wavelength of the final state contained an integral number of perturbation wavelengths. This prohibits mass transfer from one period of the equilibrium state to the next. Of course, for a definitive statement on the nature of an equilibrium state, one must consider all arbitrary perturbations. We

make additional comments on stability in §VIc.

VI. FINAL STATES

We chose several pairs of unstable wavelengths (λ_x, λ_y) for the perturbation applied to the initial state (see §III), and for each such pair we found a final equilibrium state. Figures 2a, 2b, and 2c represent typical final states, produced by perturbations that had the same vertical but different horizontal wavelengths. Ten field lines (solid curves) and three isodensity contours (dashed lines) are shown. The field lines are chosen so that the amount of magnetic flux contained between any two consecutive ones is constant. Thus, the spacing between consecutive field lines is inversely proportional to the mean strength of the magnetic field in the interval. The ratio α in the initial state (the only free parameter in the equations) was taken equal to unity.

a) Dependence on λ_x

A comparison of Figures 2a, 2b and 2c reveals that, as the horizontal wavelength increases, so does the deformation of the field lines. It is the case that the more deformed the field lines are, the more effective the gravitational field is in "unloading" the gas from their inflated portions. Therefore, the gas density at the midplane of the condensation ($x = 0$, $y > 0$) is expected to increase as λ_x increases. This is borne out in Figure 3, which exhibits the dependence of the "emission measures" (EM) on x, in these three final states.[2] The horizontal distance (x) is measured from the center

---

[2] We define the emission measure of a final state at a particular x by $EM(x) = \int \rho_f^2(x,y)\, dy$, and we normalize it to that of the initial state, $EM_i = \int \rho_i^2(y)\, dy$. The subscripts f and i denote final and initial states, respectively.

of each condensation. In the final state characterized by X = 15, we note that

$$EM(x=0) \simeq 3\ EM(x=15), \quad EM(x=0) = 2.2\ EM_i\ . \qquad (33),(34)$$

In this final state the column density of the gas as a function of x, $N_H(x)$, differs from EM(x) by at most 18%; in the other two final states presented, EM(x) and $N_H(x)$ differ by only a few percent.

A striking feature of the final states is the fact that, compared to the initial scale-height, the scale-height of the gas increases at the position of the magnetic field "valleys" and decreases at the "wings" of the condensations, where the field lines have expanded. At the midplane of the condensations, moreover, while the gas density increases with increasing λ_x, the scale-height of the gas increases as well (compare the lowest isodensity contours of Figures 2a, 2b, and 2c). This implies that the gas density increases not so much because of compression in the vertical direction, but because of a very efficient drainage of the gas from the inflated field lines. The additional fact that, in the "wings", the gas density and the scale-height decrease as λ_x increases, precludes the explanation that gas observed at high altitudes in the Galaxy is gas that has been lifted by the expanded field lines. In fact, if the magnetogravitational instability is to be invoked to explain the high-altitude gas, one should concentrate on the identification of that gas with the rise of the isodensity contours at the position of magnetic field "valleys" (see Figure 2).

The ratio of the magnetic-to-gas pressures, an interesting quantity in itself, constitutes another indicator of the efficiency with which gas drains down the inflated field lines, and of the dependence of this efficiency on λ_x. Table 1 exhibits the values of $\alpha(x,y)$ [see equation (13)] in the final

states of Figures 2a, 2b and 2c (heretoforth referred to as states a, b and c) at some key points (x,y). The gas density is also shown at the same points; it is normalized to its initial value on the x-axis. In addition to the information supplied in Table 1, we remark that both, the gas density and the magnetic field are monotonically decreasing functions of y at a fixed x.

Insert Table 1

At the two values of y used in Table 1, the normalized density in the initial state is $\rho_i(0) = 1.0$ and $\rho_i(22) = 1.8 \times 10^{-5}$. The final density along the x-axis is always uniform (and equal to unity to within a few percent) because of the requirement that there be reflection symmetry about the x-axis [see equation (18)]. No pressure gradients can be sustained along the x-axis, because the x-component of the gravitational field is assumed to vanish, and because magnetic forces do not act along field lines.

Both, the fact that at $x = 0$ alpha decreases monotonically as y increases, and the fact that at $x = X$ alpha increases monotonically with y, are different expressions of the same conclusion stated above, namely: the increase of the gas density in the magnetic field "valleys" is primarily due to efficient drainage along field lines, rather than due to compression perpendicular to the galactic plane. This drainage is more efficient the larger λ_x is. In addition, the computed low densities at $x = X$ and large y's, in conjunction with the large values of α in the same region, indicate that the magnetic field is nearly a vacuum field at the raised portions of the upper field lines.

The absolute "horizontal width" of the condensation (denoted by D and defined as the distance from the center of the condensation to the point x,

at which the normalized emission measure becomes equal to unity) shows an increase with increasing λ_x (see Figure 3). However, the ratio D/λ_x decreases as λ_x increases; it is equal to 0.47 in state a and drops to 0.38 in state c. We should bear in mind that the above definition of D uses as a reference the stratified initial state, which, as emphasized in §IIb, is needed only to provide a mass-to-flux ratio in each flux tube of the system. In external galaxies seen face-on, one can observe the contrast between regions of high and regions of low gas density. Thus, the relevant quantity is the ratio EM(x=0)/EM(x=X) for each of the states of Figure 3. This contrast becomes more pronounced as λ_x increases.

b) Energy Changes

In making a transition from an initial to a corresponding final state, the system alters its magnetic and gravitational energies. In addition, while remaining isothermal, the gas does work (positive or negative) against pressure forces, thus releasing or absorbing heat [see equation (29)]. The net reduction of each of the three forms of energy is shown in Table 2 in the case of the final states a, b and c. In each state all numbers are normalized to the internal energy (U) of the gas which is given by

$$U = \int \frac{3}{2} P \, dV \ . \tag{35}$$

The quantity U is constant because of the isothermal equation of state and because of conservation of total mass.

Insert Table 2

Starting with the heat term, we note that more heat is given off as λ_x

increases. Since heat is released by compressed gas and absorbed by expanded gas, the amount of heat released may be taken as a rough measure of the net compression sufferred by the gas. Thus, the entries in the second column of Table 2 confirm that, the larger λ_x is, the more efficiently the gas is compressed.

In spite of the large expansion sufferred by field lines in the "wings" of each condensation, the reduction in magnetic energy is small compared to that of the other energy terms. The relatively weak compression of the magnetic field [that takes place primarily along the midplane ($x = 0$, $y > 0$)] almost cancels the effect of the large expansion in the "wings". This is not surprising, since the field lines that suffer the greatest expansion are those at intermediate and high altitudes, where the magnetic energy content is small in the first place. The increase in the amount of magnetic energy released at larger λ_x may be due to the availability of a larger volume, in which field lines can expand.

The gravitational energy behaves as anticipated in §IVc. It is interesting to note that the heat released keeps pace with the decrease in gravitational energy, since both quantities reflect the accumulation of gas in magnetic field "valleys".

c) Which is The Final State?

Over horizontal distances that are larger than twice the critical wavelength Λ_x, given by equation (31), the possibility of two "final" states (one having a wavelength equal to twice that of the other) arises. Merely on energy considerations, the state with the longer wavelength is a more likely final state, since it is lower in total energy. We chose $Y = 25$ and $X = 18$ and we applied a perturbation to the stratified initial state that had a

wavelength $\lambda_x = X$ (rather than the usual $\lambda_x = 2X$).[3] Furthermore, we imposed

[3] Whenever numbers are given, the unit of length is C^2/g, where C is the isothermal speed of sound in the gas and g is the magnitude of the vertical gravitational field of the galaxy (assumed to be a constant; see §III).

no condition whatsoever at $x = X/2$. The final state obtained in this manner exhibited the characteristic double "hump", as expected. Its field lines differred from those of Figure 2a by less than three parts in one thousand at all points. When perturbations were applied to this state, the iterative scheme converged back to it. Only when the amplitude of the "perturbation" was so large that it erased the double "hump", did the iterative scheme picked out the state that has twice as large a horizontal wavelength. This leads us to believe that both states represent local potential wells and that it takes a finite amount of energy to push the system out of the state with the shorter wavelength and down the potential hill into the lower energy state, characterized by the longer wavelength. If perturbations that can provide the necessary energy are available, the interstellar gas condensations discussed so far may tend to coalesce into larger (and denser) condensations, separated by a larger mean distance.

Suppose, now, that a disturbance in the initial state consists of a superposition of many wavelengths. Under these conditions, which final state will be reached? A perturbation with initial growth-rate n grows in time as exp(nt). Because of the exponential dependence on n, the amplitudes of two perturbations, which differ in their growth-rates by a small amount, will be very different after some time has elapsed. So, given a spectrum of wavelengths for the initial perturbation, that final state is more likely

to be reached that has a wavelength corresponding to the maximum growth-rate. In all cases presented, we have fixed Y = 25. Since we also took $\alpha = 1$, this implies that the maximum growth-rate occurs at, approximately, X = 12.4. The solution of Figure 2b is close to this final state.

In summary, then, the factors deciding which final state will be reached are as follows. (i) If the initial perturbation is monochromatic, its wavelength alone determines the final state. (ii) If a spectrum of wavelengths is initially available, that final state will be reached which corresponds to the wavelength of maximum relative growth-rate. (iii) If disturbances continue to be present during the transition of the system, the amplitudes of these disturbances may also play a role in determining the final state. A definitive statement must await exact calculations.

d) Dependence on λ_y

Unlike the horizontal wavelength, the vertical wavelength does not affect a solution very much, provided only that $\lambda_y >> H$. For a fixed (unstable) λ_x we found that, by changing λ_y by almost a factor of 2 , a typical solution changed by much less than 1% at small y's, and by a few percent at intermediate y's. One could anticipate this insensitive dependence of a solution on λ_y, since more than 90% of the energy (per unit length along x) of the initial state resides under the altitude $y \approx 7$, and more than 50% of the energy is under $y \approx 2.5$. We further observed that the shape of the field lines at very large y's depends on λ_y, if $\lambda_y \sim \lambda_x$ (>>H).[4] In the case that

---

[4] Although this is insignificant for the problem at hand because of the energy argument just cited, the shape of field lines at high altitudes may be important in the context of cosmic-ray propagation.

$\lambda_y >> \lambda_x \sim H$, this effect becomes negligible altogether.

VII. CONCLUDING REMARKS AND COMPARISON WITH OBSERVATIONS

We have determined final equilibrium states for a model of the interstellar gas and field in the galactic gravitational field. Our solutions represent large-scale isothermal condensations of the interstellar gas in magnetic field "valleys". They should not be identified with "standard clouds", which could be produced by the magnetogravitational instability only if $\alpha >> 1$ (corresponding to a cold gas and a critical wavelength of the instability which is only a fraction of the scale-height). We find that the boundaries of the large-scale isothermal condensations are fairly diffuse. This is to be expected, since we have not allowed any "phase transitions" to occur in the manner described by Field, Goldsmith and Habing (1969). The thermal instability (Field 1965), which we have not considered here, could produce only small-scale (less than 1 pc) structure within the large-scale condensations, which the magnetogravitational instability initiates.

A distinctive feature of the final states is that condensation occurs not so much because of compression in the direction of $\vec{g}$, but because of drainage of the gas along field lines, especially at intermediate and high altitudes. As a consequence, at the midplane of the condensation, the scale-height of the gas in a final state is larger (by a factor of ~ 2) than the scale-height in the corresponding stratified initial state; at the "wings" of the condensation the opposite is true. Thus, the observed gas at high Galactic altitudes cannot be interpreted as gas lifted by expanding field lines. If at all, it should be identified with the rise of the isodensity contours in magnetic field "valleys". As a corollary, it is unlikely that any substantial material galactic halo can form by inflated field

lines. A radio halo could indeed form, however, by cosmic rays and expanding field lines in the manner described by Parker (1968b).

To compare with observations one needs to know the characteristic wavelength of a typical final state. A lower limit to this wavelength is, of course, the critical wavelength for the instability, Λ_x [see equation (31)]. Care should be taken, however, not to identify H, in the expression for Λ_x, with the observed scale-height of the gas today. The observed scale-height is representative of the final state, rather than the initial one, since the growth-time of the instability is only a few times 10^7 years. Realizing that α is a point function and that it cannot, therefore, be obtained by averaging either $\vec{B}$ or ρ over large distances, in order to make a semi-quantitative comparison with observations we assume that $\alpha \sim 1$. Then, since the observed scale-height is of the order of 10^2 pc, we expect gas condensations produced by Parker's instability to be separated by at least a few (3 or 4) hundred parsecs. Unless α is unexpectedly large, gas condensations separated by smaller distances than this cannot be attributed to this instability. Because Parker's instability is associated with very long wavelengths, final condensations involving up to 10^6 solar masses could be produced. (Note that a gas element travels only a fraction of the horizontal wavelength in going from an initial to a final state.) Also, because of the large scales that could be involved (up to a few kiloparsecs), we view this instability as providing the stage on which small-scale processes in the interstellar medium (e.g., dark cloud formation and cloud collapse, star formation and supernova explosions e.t.c.) act out their individual roles.

Both, the nicely displayed, recent 21-centimeter observations by Heiles and Jenkins (1973), as well as the compilation of 21-centimeter observations by Fejes and Wesselius (1973), when combined with the starlight polarization

measurements by Mathewson and Ford (1970), reveal an intimate association between the interstellar gas and the interstellar magnetic field. In fact, enormous gas condensations coincide with magnetic field "valleys". At the position of the field "valleys" the gas extends high above the plane and it does so in directions parallel to the magnetic field. The most prominent condensation is centered at about $\ell = 40°$; it is a few tens of degrees wide and extends above (and below) the plane by at least as much as 60°. Field lines emanating from this condensation form arches above the sun's location and return to the plane in the general direction $\ell = 250°$, where another condensation is located. The "edge" of the condensation at $\ell = 40°$ may be as close as 100 pc, and that at $\ell = 250°$ as close as 200 pc. However, the starlight-polarization maps of Mathewson and Ford show that most of the contribution to polarization comes from the distance range 200--400 pc in each of these directions. Moreover, contribution to polarization is also made by gas extending out to about 600 pc in each direction. Therefore, the separation between the "centers" of the two condensations may be as large as 600 pc. Not only is this separation within the range of unstable wavelengths for the magnetogravitational instability, but it may also be close to the wavelength corresponding to the maximum growth-rate.

Below the Galactic plane, two prominent condensations that are centered at $\ell \simeq 40°$ and $\ell \simeq 190°$, respectively, are similar in size and in separation with the ones just discussed. They, also, are located in magnetic field "valleys" and they are joined by field lines that arch high above the plane. They, too, may constitute evidence that the magnetogravitational instability has occurred in the solar neighborhood.

If Jeans' instability were responsible for the formation of these condensations, (i) they would be more centrally condensed; and (ii) the long

dimension of each condensation would certainly not be along the magnetic field. When self-gravitation becomes important, three-dimensional calculations (that incorporate the assumption of flux-freezing rigorously) show that the equilibrium states exhibit flattening along the magnetic field (Mouschovias 1974).

The observed symmetry of high- and low-density regions about the Galactic plane is understood in the context of the magnetogravitational instability. Whatever the mechanism that triggers the instability (spiral density shock waves ?), it certainly must act coherently over a region larger than the critical wavelength for the onset of the instability (several hundred parsecs). Since the interstellar gas forms a thin disk having thickness of a few hundred parsecs today, the perturbation that triggers the instability can influence the gas above and below the Galactic plane in a similar manner. If the initial distribution of the gas was symmetric about the plane, the final state is, therefore, expected to retain this symmetry. Smaller-scale deviations from this symmetry may be attributed to local phenomena (e.g., depletion of gas by star formation; ionization by nearby stars; sweeping of gas by supernova shocks, e.t.c.).

Observations of the motion of the interstellar gas in the solar neighborhood show a flow pattern in which gas falls down towards the Galactic plane and flows out in the general direction of the Galactic center and that of the anticenter (Erickson, Helfer and Tatel 1959; Helfer 1959; Weaver 1973). The velocities observed are a few kilometers per second. This particular flow pattern is consistent with a picture in which gas is still sliding down the expanding field lines joining the two condensations referred to above, which are located at $\ell \approx 40°$ and $\ell \approx 250°$.

Observations of external galaxies provide further evidence for the

magnetogravitational instability. This (and some consequences of the assumption that the instability is triggerred by a spiral density shock wave) will be discussed in another publication (Mouschovias, Shu and Woodward 1974).

VIII. ACKNOWLEDGEMENTS

It is with much appreciation that I recall the problematizing discussions which I have shared with Professor George B. Field. I am also thankful to Dr. Paul Concus for his advice on numerical matters in general, and for his help in estimating the asymptotic convergence-rate of the iterative scheme, in particular. Professor Frank H. Shu's criticism is much appreciated. Without the generosity of the Theoretical Physics Group of the Lawrence Berkeley Laboratory who provided me with time on the LBL excellent computing facilities, this project would not have been completed. I am also indebted to the Mathematics and Computing Group of LBL for their support.

APPENDIX A

GENERALIZATION OF THE FUNCTION q TO EQUATIONS OF STATE $P = P(\rho)$

Even if the isothermal equation of state is replaced by a general equation of state

$$P = P(\rho) , \tag{A1}$$

a connection between initial and final states may still be made. For this purpose we define $q(x,y)$ by

$$q = \exp\left(\int \frac{dP}{\rho} + \psi \right) . \tag{A2}$$

Following the same procedure that we did in §II we can still show that

$$q = q(A) \tag{A3}$$

and that equations (10) and (12) now become, respectively,

$$\nabla^2 A = -4\pi\rho \frac{d\ln q(A)}{dA} \tag{A4}$$

and

$$q(A) = \frac{1}{2} \frac{dm}{dA} \Big/ \int_0^X dx \frac{\partial y(x,A)}{\partial A} \left(\frac{dq}{dP} - q(A) \frac{d\psi}{dP} \right)^{-1} . \tag{A5}$$

In equation (A4) ρ is eliminated by using equation (A2), i.e.,

$$\rho = q(A) \left(\frac{dq}{dP} - q(A) \frac{d\psi}{dP} \right)^{-1} . \tag{A6}$$

In practice, the derivatives appearing in the right-hand sides of equations (A5) and (A6) are calculated in a straight-forward fashion by using the chain-rule. We obtain

$$\frac{dq}{dP} = \frac{dq}{dA}\frac{dA}{dP}$$

$$= \frac{dq}{dA}\left(\frac{\partial A}{\partial x}\frac{\partial x}{\partial \rho} + \frac{\partial A}{\partial y}\frac{\partial y}{\partial \rho} \right)\left(\frac{dP}{d\rho} \right)^{-1} \qquad \text{(A7)}$$

and

$$\frac{d\psi}{dP} = \left(\frac{\partial \psi}{\partial x}\frac{\partial x}{\partial \rho} + \frac{\partial \psi}{\partial y}\frac{\partial y}{\partial \rho} \right)\left(\frac{dP}{d\rho} \right)^{-1} . \qquad \text{(A8)}$$

The price, which we have paid in order to replace the isothermal equation of state with the general equation of state (A1), is that the iterative procedure over the single function A must now be replaced by an iterative procedure over all three functions A, q, and ρ. The solution of this general problem is feasible.

APPENDIX B

AN "ENERGY INTEGRAL" FOR AN ISOTHERMAL PLASMA

Bernstein et al. (1958) state that the equations of magnetohydrodynamics

$$\frac{d\vec{v}}{dt} = -\vec{\nabla}P - \rho\vec{\nabla}\psi + \frac{\vec{j}}{c}\times\vec{B} \tag{B1}$$

$$\frac{\partial\rho}{\partial t} + \vec{\nabla}\cdot(\rho\vec{v}) = 0 \tag{B2}$$

$$\vec{E} + (\vec{v}/c)\times\vec{B} = 0 \tag{B3}$$

$$\frac{d}{dt}(P\rho^{-\gamma}) = 0 \tag{B4}$$

$$\vec{\nabla}\times\vec{E} = -\frac{1}{c}\frac{\partial\vec{B}}{\partial t} \tag{B5}$$

$$\vec{\nabla}\times\vec{B} = (4\pi/c)\,\vec{j} \tag{B6}$$

$$\vec{\nabla}\cdot\vec{B} = 0 \tag{B7}$$

possess the energy integral

$$\int dV \left(\frac{1}{2}\rho v^2 + \frac{B^2}{8\pi} + \rho\psi + \frac{P}{\gamma-1} \right) = \text{a constant}, \tag{B8}$$

where the integration is extended over all space. The operators $\partial/\partial t$ and d/dt denote Eulerian and Lagrangian time-derivatives, respectively.

Here we show that, even in the case that the plasma is isothermal (i.e., $\gamma = 1$), an "energy integral" still exists; it is identical with that of equation (B8), except for the fact that the term $P/(\gamma-1)$ is replaced by $P\ \ln P$. We procede in the usual manner to take the dot product of both sides of equation (B1) with $\vec{v}$; then, by using equations (B2)-(B7), we write each

term as follows.

$$\vec{v}\cdot\frac{\vec{j}}{c}\times\vec{B} = -\vec{\nabla}\cdot\left(\frac{c}{4\pi}\vec{E}\times\vec{B}\right) - \frac{\partial}{\partial t}\left(\frac{B^2}{8\pi}\right) , \tag{B9}$$

$$-\rho\vec{v}\cdot\vec{\nabla}\psi = -\vec{\nabla}\cdot(\rho\psi\vec{v}) - \frac{\partial}{\partial t}(\rho\psi) . \tag{B10}$$

Also,

$$-\vec{v}\cdot\vec{\nabla}P = -\vec{\nabla}\cdot(P\vec{v}) + P\,\vec{\nabla}\cdot\vec{v} . \tag{B11}$$

But, by judiciously adding and subtracting the quantity $P\ \ln P\ \vec{\nabla}\cdot\vec{v}$, we can show that the last term in equation (B11) may be written as

$$P\,\vec{\nabla}\cdot\vec{v} = -\left[\frac{\partial}{\partial t}(P\ \ln P) + \vec{\nabla}\cdot(P\ \ln P\ \vec{v})\right] . \tag{B12}$$

Collecting all terms we obtain

$$\begin{aligned}&\frac{\partial}{\partial t}\left(\frac{1}{2}\rho v^2 + \frac{B^2}{8\pi} + \rho\psi + P\ \ln P\right)\\ &+\vec{\nabla}\cdot\left(\frac{1}{2}\rho v^2\,\vec{v} + \frac{c}{4\pi}\vec{E}\times\vec{B} + \rho\psi\vec{v} + P\ \ln(P/e)\,\vec{v}\right) = 0 .\end{aligned} \tag{B13}$$

In equation (B13), e is the natural-logarithm base. If the plasma extends over all space, being periodic in x (with a wavelength λ_x) and symmetric about the x-axis, we may integrate equation (B13) over one period of the system in x, and over the upper half plane in y.† The divergence term yields

---

† As in the main text, the geometry is taken to be two-dimensional, although this is not necessary for this argument.

---

a surface integral with all the terms vanishing, if there is no mass transfer

from one period to the next, or across the x-axis, and if either the magnetic field or the velocity vanishes at $y = \infty$. Formally these conditions are

$$\hat{n}\cdot\vec{v} = 0 \quad \text{at} \quad \begin{cases} (x,\ y = 0) \\ (x = \pm X,\ y) \end{cases} \tag{B14}$$

and either

$$\vec{B}(x,\ y = \infty) = 0, \quad \text{or} \quad \vec{v}(x,\ y = \infty) = 0. \tag{B15}$$

The unit normal to the "surface" of a period is denoted by $\hat{n}$, and X is equal to $\lambda_x/2$. Thus, the result of the integration is

$$\int dV \left(\frac{1}{2}\rho v^2 + \frac{B^2}{8\pi} + \rho\psi + P\ \ln P \right) = \text{a constant.} \tag{B16}$$

The first term in this integral is the kinetic energy of the fluid. The sum of the other three terms acts as an effective potential energy of the isothermal plasma. This point and the meaning of $P\ \ln P$ are discussed in the main text (see §IV). Here we only remark that $P\ \ln P$ is not the internal energy density of the fluid; the latter is always equal to $3P/2$.

APPENDIX C

METHOD OF SOLUTION

1) The Dimensionless Problem

We measure the magnetic vector potential and the gas density in units of their initial values on the x-axis, i.e., $-2HB_i(0)$ and $\rho_i(0)$, respectively. The unit of length is taken as C^2/g and the unit of time is fixed by choosing the unit of velocity as C, the isothermal speed of sound in the gas. With the gravitational field chosen as in §III, we may write the dimensionless form of equation (10) as

$$\nabla^2 A(x,y) = Q(y,A;\alpha) \ , \tag{C1}$$

where

$$Q(y,A;\alpha) = -\frac{1}{8\alpha(1+\alpha)^2}\frac{dq(A)}{dA}\exp(-y) \ . \tag{C2}$$

The parameter α is characteristic of the initial state [see equation (13)]. Similarly, equation (12) becomes

$$q(A) = \frac{1}{2}\frac{dm}{dA} \Big/ \int_0^X dx \, \frac{\partial y(x,A)}{\partial A} \exp[-y(x,A)] \ , \tag{C3}$$

where

$$\frac{dm}{dA} = -4X(1+\alpha)A \tag{C4}$$

and X is defined by $X \equiv \lambda_x/2$. The dimensionless form of the boundary conditions is

$$A(x,y=0) = 1, \tag{C5}$$

$$\frac{\partial A(x,y)}{\partial x}\Big|_{x=0,\pm X} = 0 \ , \tag{C6}$$

and

$$A(x,y) = \begin{cases} 0, & y = +\infty \\ 2, & y = -\infty \end{cases} . \qquad (C7)$$

The approximate boundary condition that replaces equation (C7) is

$$A(x,y) = A_i(Y) , \qquad (C8)$$

with $A_i(y)$ given by

$$A_i(y) = \exp[-y/(2\alpha+2)] . \qquad (C9)$$

2) Outline of the Numerical Scheme

In equation (C1) ∇^2 is a linear, differential operator and Q is a non-linear, algebraic operator. We solved equation (C1) numerically by an under-relaxation iterative procedure. The premise was that, if we can calculate Q as a function of x and y (rather than A and y), we could easily solve the resulting Poisson equation by any one of the many available fast techniques (see Dorr 1970). We know Q as a function of x and y, however, only if a solution A(x,y) is at hand; hence the necessity of an iterative scheme.

Starting from an initial guess $A^{(0)}(x,y)$, we define a sequence of iterates by the recursion relations

$$\nabla^2 A^{*(n+1)} = Q(y, A^{(n)}; \alpha) , \qquad n = 0, 1, 2, \ldots \qquad (C10)$$

$$A^{(n+1)} = \theta^{(n)} A^{(n)} + (1-\theta^{(n)}) A^{*(n+1)} , \quad 0 \leq \theta^{(n)} < 1 . \qquad (C11)$$

The quantity $A^{*(n+1)}$ is a provisional iterate and $\theta^{(n)}$ is the relaxation parameter at the nth iteration. We say that a solution is reached, if the following condition is satisfied at all points (x,y):

$$\left|\frac{\overset{*}{A}^{(n+1)} - A^{(n)}}{\overset{*}{A}^{(n+1)}}\right| < \varepsilon \ . \qquad \text{(C12)}$$

In equation (C12), absolute values are denoted by $|\ |$. (Recall that the dimensionless A is always positive.) The quantity ε is a small positive number and can be chosen at will to achieve desired levels of accuracy.

We chose some field lines of the initial state (the number varied from 65 to 129), we introduced perturbations most often having the form

$$\delta A(x, y) = - A_i(y)\ \mu\ \sin(\pi y/Y)\ \cos(\pi x/X) \ , \qquad \text{(C13)}$$

where μ is a fixed positive number less than unity, and we followed these field lines from iteration to iteration until they settled down. Although we found solutions (to within 1% or 2%) in a number of iterations varying from 6 to 22, we forced the program to continue for as many as 97 iterations in order to make a detailed error analysis. Thus, we computed the asymptotic convergence rate and demonstrated that, at any one interior point, our solutions are accurate to within 0.5%.

In more detail, the steps involved in the iterative scheme are the following.

(i) Define a uniform mesh over the region of interest having J points in the y- and K points in the x- directions:

$$y_j = (j-1)\ \Delta y \ , \quad j = 1, 2, \ldots J \ ; \qquad \text{(C14)}$$

$$x_k = (k-1)\ \Delta x \ , \quad k = 1, 2, \ldots K \ ; \qquad \text{(C15)}$$

where $\Delta y = Y/(J-1)$ and $\Delta x = X/(K-1)$. [Note that having defined a mesh, all functions of one (two) variables become one- (two-) dimensional arrays.]

(ii) Choose a set of field lines of the initial state which we shall follow. Let this set be $\{A_i\}$, $i = 1, 2, \ldots I$.

(iii) Guess an $A^{(0)}(x,y)$.

(iv) For each x, interpolate to find $y(A_i,x)$, i = 1, 2, ... I. That is, obtain y as a function of x along each field line chosen in step (ii).

(v) For each x, differentiate $y(A_i,x)$ with respect to A to obtain $\partial y/\partial A$.

(vi) Perform the integration in equation (C3) for each and every A_i.

(vii) Obtain $q(A_i)$ from equation (C3), since $dm(A_i)/dA$ is always given by equation (C4).

(viii) Perform the differentiation with respect to A to find $h(A_i) \equiv dq(A_i)/dA$.

(ix) Since $h(A_i)$ is known along the field lines, whose position was determined in step (iv), interpolate to obtain h at the mesh points. This interpolation is done, for each x, by using $y(A_i,x)$ as old abscissas and y_j as new abscissas; the subscripts i and j span their respective ranges.

(xi) With the right-hand side known as a function of x and y, the Poisson equation (C1) is solved to find $A^{(1)}(x,y)$.

(xii) If $A^{(1)}$ and $A^{(0)}$ satisfy the criterion given by equation (C12), then $A^{(1)}$ is a solution. If they do not, underrelax A as in equation (C11) and go back to step (iv) to repeat the process.

Numerical integrations, differentiations and interpolations are performed so many times in the program that, although the routines performing each operation are very accurate, their combined effect in the calculation of the right-hand side of equation (C1) cannot be predicted. To study this effect we searched for a function $\bar{A}(x,y)$, which would (i) correspond to field lines having the desired wavy shape; (ii) satisfy the appropriate boundary conditions; and (iii) allow us to calculate the right-hand side of equation (C1) analytically! If such an $\bar{A}(x,y)$ is known, then the calculated $Q(y,\bar{A};\alpha)$ can be compared to the Q computed by the program and the net

numerical errors be determined. Such an $\bar{A}$ is obtained by solving the quadratic

$$\exp[- y/(2\alpha+2)] = (1-\bar{A})\ (\bar{A}-A_o)\ w(x) + \bar{A}\ , \qquad (C16)$$

where

$$w(x) = \kappa \cos(\pi x/X)\ , \quad |\kappa| < 1 \qquad (C17)$$

and A_o is the value of A in the initial state at $y = Y$.

It is remarkable that we found that the maximum error in the computation of $dq(\bar{A})/dA$ occurs at the upper boundary (where all physical quantities are very small compared to their values on the x-axis) and is equal to 0.91%. Table 3 exhibits the maximum errors in the computation of the various quantities and the points at which these errors occur. The mesh was uniform in each direction; the number of mesh points in the y-direction was 65 and that in the x-direction was 63. This is the smallest number of mesh points used to obtain any one of our solutions. Thus, the errors given in Table 3 are the largest that we may expect. The indices j and k denote mesh points in the y- and x- directions, respectively [see equations (C14) and (C15)]. The index i denotes field lines, the lowest field line having $i = 1$ and the one at $y = Y$ having $i = 65$.

Insert Table 3

Note that the maximum errors occur at the boundaries. In fact, the errors at interior points are much less than those given in Table 3.

TABLE 1

ALPHA AND THE GAS DENSITY IN THREE FINAL STATES[1] AT SOME POINTS

(x,y)	α(x,y)			ρ(x,y)		
	a	b	c	a	b	c
(0,0)	1.2	1.4	2.0	1.0	1.0	1.0
(0,22)	0.1	0.05	0.03	8.8×10^{-5}	2.1×10^{-4}	4.2×10^{-4}
(X,0)[2]	0.9	0.7	0.6	1.0	1.0	1.0
(X,22)	1.6×10^{2}	7.1×10^{3}	9.0×10^{4}	1.8×10^{-6}	1.8×10^{-7}	4.1×10^{-8}

[1] The columns headed a, b and c refer to the final states of Figures 2a, 2b and 2c.

[2] Recall that X ($\equiv \lambda_x/2$) is different in each state; it increases as we go from state a to state c.

TABLE 2

ENERGY REDUCTION FOR THREE FINAL STATES

Final State	Energy Released [1]		
	Heat ($\times 10^2$)	Magnetic ($\times 10^2$)	Gravitational ($\times 10^2$)
a	2.32	0.00	2.37
b	5.73	0.90	5.50
c	11.8	2.67	12.9

[1] In each state, the energy released has been normalized to the internal energy of the gas, $\frac{3}{2} \int P \, dV$.

TABLE 3

MAXIMUM COMPUTATIONAL ERRORS

Function	Maximum Error (%)	Location
$y(\bar{A},x)$	0.320	i = 2, k = 2
$\frac{\partial y(\bar{A},x)}{\partial A}$	0.060	i = 65, k = 15
$f(\bar{A})$ [1]	0.098	i = 1
$q(\bar{A})$	0.445	i = 65
$\frac{dq(\bar{A})}{dA}$	0.770	i = 64
$\frac{dq[\bar{A}(x,y)]}{dA}$	0.91	j = 64, k = 45

[1] The function $f(\bar{A})$ is defined as the integral in the denominator of equation (C3).

REFERENCES

Bernstein, I. B., Frieman, E. A., Kruskal, M. D. and Kulsrud, R.M. 1958, Proc. Roy. Soc. (London), A244, 17.

Dorr, F. W. 1970, SIAM Review, 12, No. 2, 248.

Dungey, F. W. 1953, Monthly Notices Roy. Astron. Soc.. 113, 180.

Erickson, W. C., Helfer, H. L. and Tatel, H. E., 1959, IAU Symp. 9, 390.

Fejes, I. and Wesselius, P. R. 1973, Astron. & Astroph., 24, No. 1, 1.

Field, G. B. 1965, Ap. J., 142, 531.

Field, G. B., Goldsmith, D. and Habing, H. J. 1969, Ap. J. Lett., 155, 149.

Heiles, C. and Jenkins, E. 1973, papers presented at 139th and 140th meeting of Am. Astron. Soc., and IAU Symp. No. 60.

Helfer, H. L. 1959, A. J., 64, 128.

Lerche, I. 1967a, Ap. J., 149, 395.

_____. 1967b, Ap. J., 149, 553.

Mathewson, D. S. and Ford, V. L. 1970, Memoirs Roy. Astron. Soc., 74, 143.

Mouschovias, T. Ch., Shu, F. H. and Woodward, P.R. (submitted to A&A)

Mouschovias, T. Ch. 1974 (in preparation).

Parker, E. N. 1966, Ap. J., 145, 811.

_____. 1968a, Ap. J., 154, 57.

_____. 1968b, in Stars and Stellar Systems, vol.VII,(Chicago: The Univ. of Chicago Press) pp. 707-754.

Schmidt, M. 1965, in Stars and Stellar Systems, vol. V, (Chicago: The Univ. of Chicago Press) pp.513-530.

Spitzer, L. Jr. 1968, Diffuse Matter in Space, (New York: Interscience).

Weaver, H. 1973, paper presented at the IAU Joint Discussion No. 3, Sydney, Australia.

CAPTIONS TO FIGURES

Fig. 1 - The dependence of the function q on A in the stratified initial state ($\alpha = 1$) and in a typical final state (that of Figure 2c). Both q and A are normalized to their values on the x-axis in the initial state.

Fig. 2a (left), 2b (center), and 2c (right). - Final equilibrium states of the interstellar gas-field system in a galactic gravitational field $\vec{g} = -\vec{e}_y\, g(y)$, where $g(y) = -g(-y) =$ a positive constant. Distance is measured in units of C^2/g, where C is the isothermal speed of sound in the gas. The dimensions of each graph are equal to half a wavelength in the x- and half a wavelength in the y-direction. Half the critical wavelength in the x-direction is equal to 7.26. Field lines (solid curves) are chosen so that the magnetic flux between any two consecutive ones is constant. The isodensity contours (dashed curves) represent the points at which the density decreases to e^{-1}, e^{-2} and e^{-3} its value on the x-axis. The number on each curve is the y-coordinate of that curve in the initial state, in which $\alpha = 1$.

Fig. 3 - The emission measure (normalized to its value in the stratified initial state) as a function of x in the three final states of Figure 2. The unit of length is C^2/g. The number (X) labeling each curve is equal to 1/2 of the horizontal wavelength of the corresponding final state. The curves X = 9 and X = 12 could also represent the normalized column density in the corresponding final states to within a few percent. Similarly, the curve X = 15 could represent the corresponding column density to within 18%.

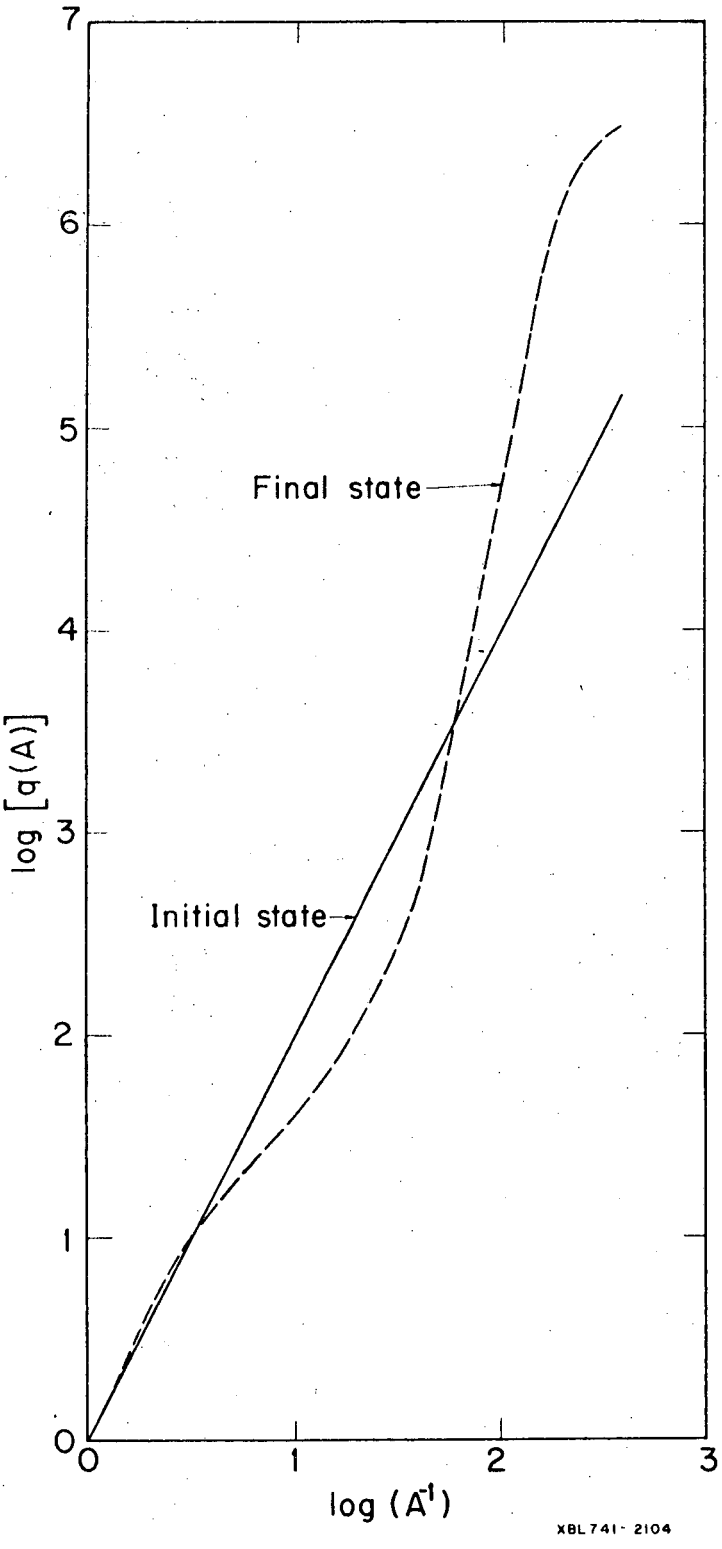
7
6
5
4
3
2
1
0
0
1
2
3
log [q(A)]
log (A⁻¹)
Final state
Initial state
XBL741-2104

Fig. 1.

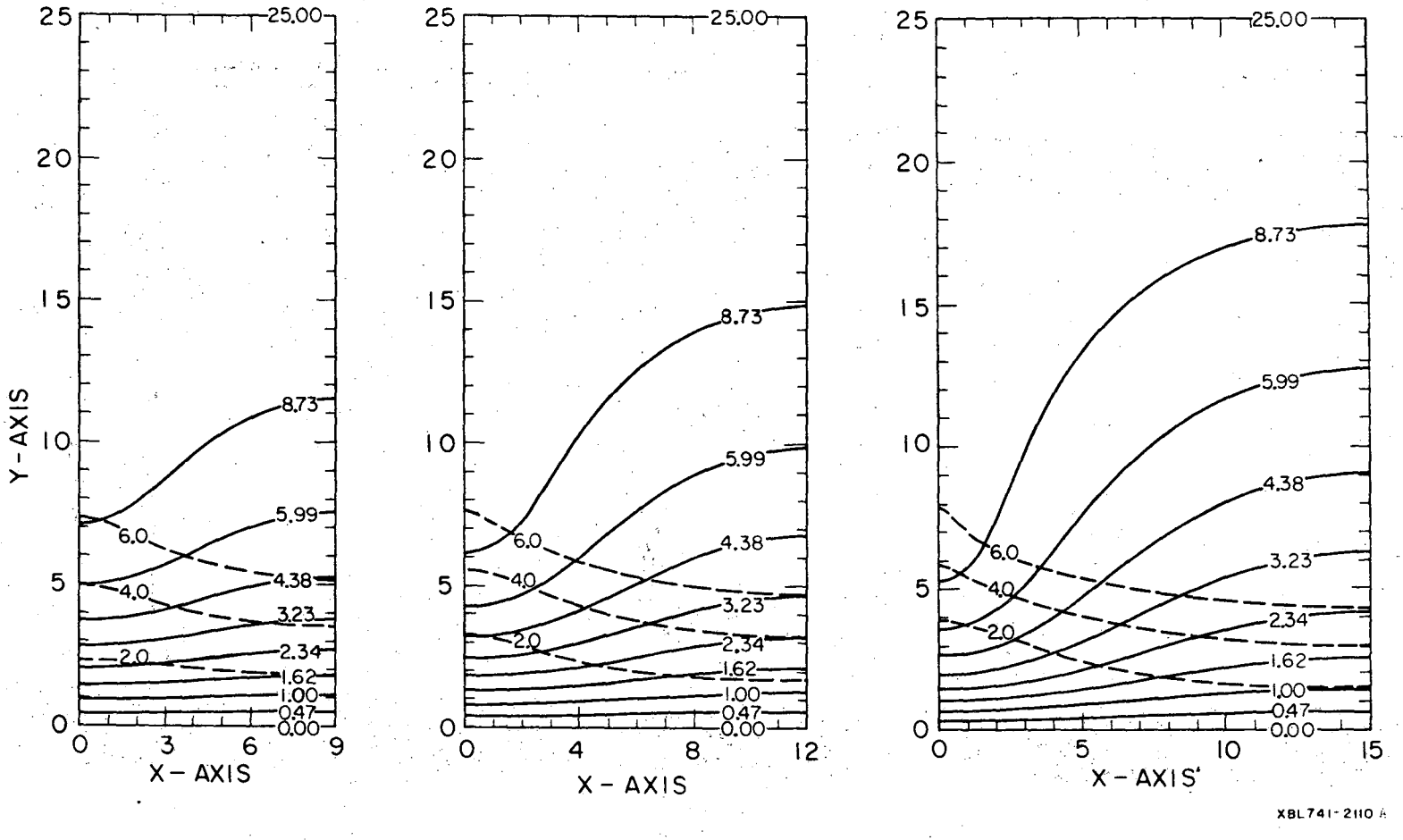
Y-AXIS
X-AXIS
25.00
8.73
5.99
6.0
4.38
4.0
3.23
2.34
2.0
1.62
1.00
0.47
0.00
XBL741-2110 A

Fig. 2.

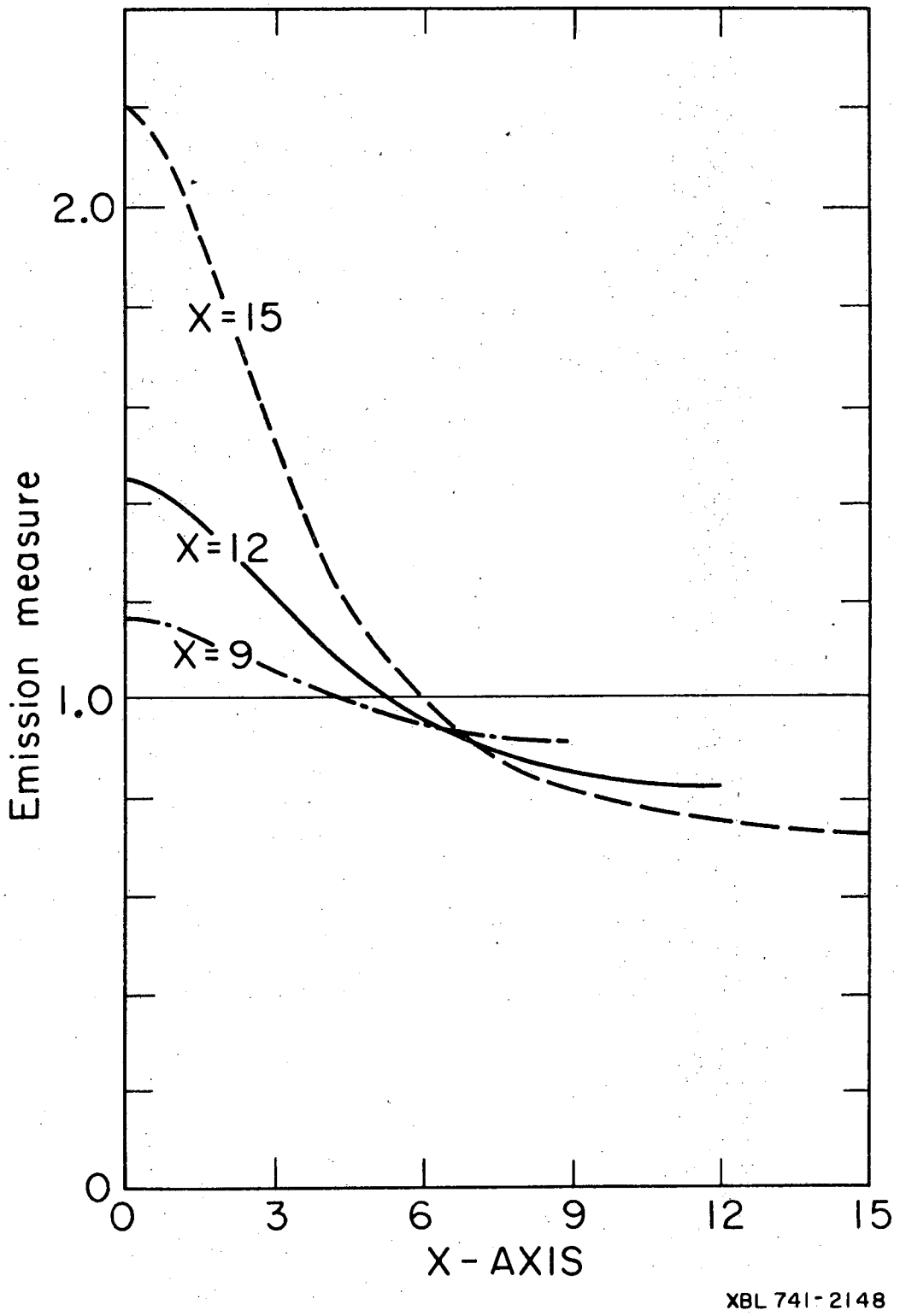
2.0
1.0
0
Emission measure
X=15
X=12
X=9
0
3
6
9
12
15
X-AXIS
XBL 741-2148

Fig. 3.

LEGAL NOTICE

This report was prepared as an account of work sponsored by the United States Government. Neither the United States nor the United States Atomic Energy Commission, nor any of their employees, nor any of their contractors, subcontractors, or their employees, makes any warranty, express or implied, or assumes any legal liability or responsibility for the accuracy, completeness or usefulness of any information, apparatus, product or process disclosed, or represents that its use would not infringe privately owned rights.

TECHNICAL INFORMATION DIVISION
LAWRENCE BERKELEY LABORATORY
UNIVERSITY OF CALIFORNIA
BERKELEY, CALIFORNIA 94720